Developing a Novel, Precision Bio-Printed, Three-Dimensional Multi-Cellular Model Mimicking the Tumour Stroma for High-Throughput Drug Response Modelling in Hepatocellular Carcinoma

By

Abdullrahman Abdullah Alnmari*

* Laboratory supervisor, Medical Cities Program – MOI, Riyadh. Saudi Arabia

Abstract- Objective: Hepatocellular carcinoma (HCC) is a major public health problem causing significant morbidity and mortality due to increasing prevalence and limited treatment options. Crosstalk between cancer cells and cells in the tumour microenvironment including cancer-associated fibroblast (CAFs) and macrophages aid cancer development, metastasis, and drug resistance to standard therapies such as Sorafenib. Effectively modelling these interactions in of primary importance to develop novel treatments. Researcher aimed to develop a new bio-printed HCC model that more accurately models the microenvironment and includes interactions between HCC cells and CAFs.

Methods: Researcher used human SNU-449 HCC cells to model cancer cells, and LX-2 human myofibroblasts to model CAFs. he assessed responses to Sorafenib in two- and three-dimensional (3D) culture in the non-defined matrix BME2, and novel bio-printed 3D models using defined matrices developed by Inventia Life Sciences.

Results: Researcher established the effects of Sorafenib on SNU-449 and LX-2 cells viability in 2D model, therefore researcher compared Sorafenib effects between 2D and 3D (BME-2) models and established significance reduction on both SNU-449 and LX-2 cells viability. Then established Sorafenib effects in 3D BME-2 matrix & 3D bio-printed versus 2D using bio-printer on SNU-449 and established significance reduction of SNU-449 viability. Based on that researcher established effect of Sorafenib concentration on a multi-cellular model SNU-449 & LX-2 cells combined that mimic tumor stroma in 3D BME-2 matrix & 3D bio-printed versus 2D on inert and on plastic using bio-printer and significance reduction was observed on SNU-449 & LX-2 cells combined.

Significance: In this study, researcher successfully developed a new bio-printed HCC model by co-culturing SNU-449 cells (human HCC line) and LX-2 cells (human HSC line) and tested the effect of increase concentration Sorafenib in 2D Vs 3D using RASTRUM bio-printer.

Keywords: Hepatocellular Carcinoma, Cell Interaction, Hepatic Stellate Cell, Cancer Cells, Organoids, Tumor Microenvironment, Drug Resistance

Introduction :

Liver cancer is the third leading cause of death to malignancy worldwide (Sung et al., 2021). The major subtypes of primary liver cancer (PLC) are hepatocellular carcinoma (HCC; 85-90% of cases), which resembles hepatocyte-like cells and cholangiocarcinoma (CCA; 10-15% of cases), which resemble the bile duct epithelium. (Nuciforo, S., & Heim, M. H., 2020). Liver cirrhosis is the most common risk factor for malignancy, with common aetiologies including chronic hepatitis infections such as hepatitis B (HBV) and C (HCV) and fatty liver disease caused by alcohol consumption or metabolic risk factors (obesity, type 2 diabetes, and metabolic syndrome (McGlynn et al., 2021) (Gomaa et al., 2008). Generally, chronic liver inflammation is a key factor in the development of HCC, which leads to fibrosis and cirrhosis (Li et al., 2017). HCC incidence rates are increasing globally consequently leading to substantial morbidity and mortality thus it is a major public health problem (Dasgupta et al., 2020). Every year, over a million people are diagnosed with PLC, and 830,000 die as a result (Nuciforo, S., & Heim, M. H., 2020).

In response to liver damage, the liver can regenerate itself and make new cells. However, persistent inflammation in chronic liver inflammation leads to disruption of liver tissue and interferes with liver homeostasis causing hepatocyte death. Liver injury triggers activation and proliferation of hepatic stellate cells (HSCs) through cytokines and growth factors secreted by resident cells including Kupffer cells (KCs), hepatocytes, leucocytes, and platelets (Seki, E., & Schwabe, R. F., 2015). Kupffer cells (KCs), also known as resident hepatic macrophages, play important roles in the pathogenesis of chronic liver inflammation. Kupffer cells reside within the lumen of liver sinusoids, and in response, to liver injury, macrophages become activated to a pro-inflammatory subtype, also known as 'M1-like' macrophages (Li et al., 2017).

The balance of two types of macrophages Kupffer cells, pro-inflammatory macrophages (M1-like), which initiate the inflammatory response to liver injury and recruit monocyte-derived macrophages from the circulation, and pro-resolution macrophages (M2-like) which support liver scar breakdown and regeneration regulate chronic liver inflammation (Dwyer et al., 2021).

Macrophages carry out a variety functions, including growth factor and cytokine secretion, phagocytosis, antigen presentation, and immune control.

Macrophages secrete cytokines and chemokines such as transforming growth factor (TGF)-β, platelet-derived growth factor (PDGF), tumour necrosis factor (TNF)-α, interleukin (IL)-1β, and chemokine C-C motif ligand 2 (CCL2) driving the activation of HSCs. As chronic hepatitis induces fibrosis through activation of quiescent HSCs that differentiate into myofibroblasts, which produces extracellular matrix (ECM) components such as collagen, which form the liver scar. Activated cells express a high level of alpha-smooth muscle actin (α-SMA) therefore indicating the progression of fibrosis. Excessive ECM deposition contributes to the scarring of tissue resulting in pathological cellular functions that promote the progression of fibrosis leading to cirrhosis, and eventually HCC (Arriazu et al., 2014).

Sustained HSC activation aids in fibrosis progression and release of proinflammatory, fibrogenic cytokines and epithelial-mesenchymal transition (EMT) which contributes to creating a tumour microenvironment (TME) (Elpek G. Ö. 2014). Along with cell-cell interaction via an autocrine and paracrine mechanism in promoting tumour progression, and tumour microenvironment (TME) induced drug resistance (Cadamuro et al., 2017).

The TME plays a pivotal role in cell recruitment leading to the growth, invasion, and metastasis of tumour that induces drug resistance. Tumour stroma is composed of angiogenic factors (VEGF), growth factors (fibroblasts), immune cells, cytokines, and chemokines that have roles in the development and progression of HCC (Hernandez-Gea et al., 2013) (Hou et al., 2018). The TME is favorable for HCC cells to acquire abnormal phenotypes and attracts immune cells such as macrophages and T cells (Ringelhan et al., 2018). '

The crosstalk with tumor-associated macrophages (TAMs), cancer-associated fibroblasts (CAFs), and cancer cells affect drug treatment within TME, resulting in tumour progression and drug resistance in HCC (Bu et al., 2020) (Gunaydin G., 2021).

Tumour associated macrophages (TAMs) play a significant role in tumour progression, angiogenesis, immunosuppression, and metastasis inducing chemoresistance (Dallavalasa et al., 2021). Pro-inflammatory macrophages seem to inhibit early HCC carcinogenesis by activating adaptive immune cells which recognize and attack cancer cells (Vannella, K. M., & Wynn, T. A., 2017).

However, when the HCC tumour progress, macrophages undergo a phenotypic change from pro-inflammatory to immune-suppressive TAMs (Prieto et al., 2015). TAMs promote cancer cell proliferation and invasion and inhibit immune surveillance by suppressing the adaptive immune system (Yang et al., 2020). Additionally, TAMs contribute to suppressing the anti-tumour response that occurs throughout the development and progression of HCC, promoting chemoresistance (Krenkel, O., & Tacke, F., 2017).

The HCC tumour stroma is mainly composed of CAFs that favor cancer progression and therapeutic resistance (Wu et al., 2021). CAFs have heterogenic and diverse origins from various cell types including stellate cells, endothelial cell, epithelial cell, vascular smooth muscle cells, mesenchymal stem cells, adipocytes, and bone marrow-derived cells (Farzaneh et al., 2021) (Kanzaki et al., 2021).

Numerous studies have reported CAFs facilitating tumorigeneses and angiogenesis by creating a proinflammatory and immunosuppressive TME via interactions with cancer cells (Feng et al., 2022) (Liu et al., 2021). CAFs have critical roles in extracellular matrix remodeling and secreting a variety of growth factors, cytokines, and chemokines regulate cancer survival such as TGF-β, VEGF, hepatocyte growth factors (HGF) (Linares et al., 2021) (Liu et al., 2019).

A major obstacle to the advancement of drug development is the lack of an appropriate cell culture model system. In the advanced HCC stage, the treatment options are systemic targeted agents like multi-kinase inhibitor Sorafenib, trans-arterial chemoembolization, liver transplantation, and surgical resection, (Kumari et al., 2018). But due to the TME and its heterogeneity, the efficacy of treatments varies in patients (Tang et al., 2020). Since HCC is a complex disease that needs personalized treatment, developing models that incorporate this complexity would greatly aid in drug discovery.

Organoids can be used to model the three-dimensional (3D) structure of an organ in vitro. A wide range of applications is suitable for using three-dimensional (3D) organoid culture in disease modeling, for instance, liver cancer organoid that replicates the derived tumour genetically and histologically (Nuciforo, S., & Heim, M. H., 2020).

In contrast, using mouse models in the conventional two-dimensional (2D) culture has been a very useful method but inability to mimic the in vivo of TME (Ayvaz et al., 2021). Organoids possess several advantages such as ease, long-term expansion, and cryopreservation and three-dimensional structure that resembles the native organ, incorporating factors such as cell-cell interaction, cell movement, and cell differentiation (Balakrishnan et al., 2020). However, current organoid systems for assessing drug responses do not incorporate elements of the TME and use non-defined matrices for culture such as Matrigel or basement membrane extract (BME2), which don't model the tumour environment (Ayvaz et al., 2021). Developing new systems that incorporate stromal cells, such as CAFs, and defined matrices that more accurately model the TME would improve drug response modelling. Therefore, in this study, researcher sought to develop a multi-cellular in vitro model of HCC in defined matrices for use in high-throughput drug screening.

MATERIALS AND METHODS:

Thawing Cells (LX-2 & SNU-449), SNU-449 cells (human HCC line) (Park et al., 1995) and LX-2 cells (human HSC line) (Xu et al., 2005) were thawed at 37 °C for 1 minute. T cells were transferred and mixed with 4 ml maintenance media (89% High glucose DMEM (Thermofisher), 10% fetal bovine serum (FBS; Gibco) and 1% penicillin/streptomycin (Gibco)) in a 15 ml centrifuge tube. Cells were centrifuged at 300 x g for 5 minutes at room temperature. The supernatant was aspirated, the cells resuspended in 5 ml maintenance medium and transferred to a T25 flask (Thermo Scientific). Cells were maintained at 37°C, 5% CO_2 and 90% humidity.

Cell maintenance and sub-culturing:

For cell maintenance, medium was changed twice weekly until cells reached 80% confluence. For sub-culturing, cells were washed twice in phosphate buffered saline (PBS; Gibco) and dissociated in 1 ml Trypsin-EDTA 0.05% solution (Gibco). Dissociated cells were resuspended in 5 ml PBS, centrifuged at 300 x g for 5 minutes at room temperature and the supernatant discarded. Cells were resuspended in 1 ml maintenance medium, and then split at a ratio of 1:4 and replated into T25 flasks. LX-2 cells were used between passages 46 to 51, and SNU-449 cells at passages 5-10.

Three-dimensional cell models:

For non-defined three-dimensional cell models, 40 µl Basement Membrane Extract 2 (BME-2; In vitro technologies) was added per well of a 96-well plate and allowed to solidify for 30 minutes at 37 °C. Cells were then plated as described below in 100 µl maintenance medium on top of the BME-2. For bio-printed models, the RASTRUM bio-printer (Inventia Life Science) was initialized using the greenlighting procedure according to manufacturer instructions. Cells were printed into matrix Px02.40 (~1.1 kPa, containing GFOGER, RGD, Hyaluronic Acid). RASTRUM reagents (1.3 mL bio-ink F32, 200 µl bio-ink F264 and 1.3 mL activator F3) were thawed at room temperature. Then all reagents that specifically structured by RASTRUM software (Inventia Life Science) were added into the respective reservoirs of the RASTRUM cartridge and inserted into the printer beside well plate to print the inert base. After the inert base completed printing, researcher prepared the cell-laden ink by mixing 620,000 of SNU-449 (6,250,000 cells/ml) of SNU-449 and LX-2 at the ratio of (1:3) for 2000 cells per well in 200 µl of the activator for both experiments and transferred into the specific structured cartridge position and added 150 µl of maintenance medium to 2D control wells in the well plate in a biosafety cabinet. RASTRUM cartridge and well plate returned to the printer to print bio-functional matrix. Once completed researcher added 100 µl of maintenance medium to the 3D cell models and incubated at 37 °C, 5% CO_2 and 90% humidity.

Sorafenib response assay :

After overnight incubations DMSO was used as a control and was prepared and mixed with media at the concentration of 8ml medium and 80 µl DMSO. Sorafenib (Tocris Bioscience) was diluted at 0, 5, 10, 20, 50 µM, with the DMSO concentration consistently maintained. 100 µl drug treatments were added per well, for a final volume of 200 µl, and were incubated for three days. After 72 hours of drug incubation, 100 µl of Cell Titer Blue (for 2D experiments; Promega) or Cell Titer Glo3D (for studies involving 3D cultures; Promega) reagent was added to cultures and incubated for 30 minutes at room temperature, and fluorescence (Cell Titer Blue) or luminescence (Cell Titer Glo3D) read on a PerkinElmer EnSight plate reader according to manufacturer instructions.

Statistical analysis:

Quantitative data were expressed as mean ± standard error (SEM) using Prism v9.3.1 software (GraphPad software) after calculating the fold change. For comparison of multiple groups, a one-way ANOVA with Tukey's multiple comparisons test was used. For data with two categorical variables, a two-way ANOVA with Tukey's multiple comparisons test was used. Values were considered statistically significantly different when $p<0.05$.

RESULTS:

Establishing Sorafenib concentration in 2-D:

To establish a multi-cellular model of HCC, researcher utilized SNU-449 human HCC cells as our cancer cell model, and LX-2 human liver myofibroblasts to model CAFs. To inform our drug-response assays, researcher aimed to establish a concentration range of the drug Sorafenib, that would reduce cell SNU-449 and LX-2 viability. SNU-449 HCC line and LX-2 were seeded individually at density of 2000 cell per well in 96-well plates. After overnight incubation cells were treated with 5, 10 20 or 50 µM Sorafenib dissolved in DMSO (0.5%). Cells treated with DMSO (0.5%) were used as a vehicle control for the experiment. After 72 hours of treatment, cell viability was assessed. In SNU-449 cells, researcher observed a reduction in viability of 48.8% (5 µM), 52.1% (10 µM), 52.3% (20 µM) and 55.6% (50 µM) treatment with Sorafenib (Figure 1A). In LX-2 cells, researcher observed a reduction in viability of 51.8% (5 µM), 62.6% (10 µM), 61% (20 µM) and 60.4% (50 µM) treatment with Sorafenib (Figure 1B). Researcher successfully established that the concentration of Sorafenib between 5 and 50 µM significantly reduced SNU-449 and LX-2 viability. Researcher therefore utilized this concentration range of Sorafenib for subsequent experiments.
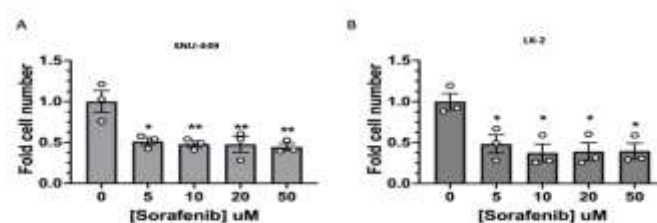

Figure 1. Effects of increase Sorafenib concentration on SNU-449 in 2-dimensional (2D) model. Cells were seeded and grown on plastic cell culture wells and treated with increasing concentrations of Sorafenib for 72 hours. Viability was quantified using CellTiter Blue reagent. **(A)** shows the reduction of SNU-449 cells viability in increasing concentration of sorafenib as shows to inhibit cell viability. Data are presented as a fold change over vehicle control and represent mean ± SEM (n=3). One way ANOVA with Tukey's post-test (n=3). *$p<0.05$, **$p<0.01$. **(B)** shows the reduction of LX-2 cells viability in increasing concentration of sorafenib as shows to inhibit cell viability. Data are presented as a fold change over vehicle control

and represent mean ± SEM (n=3). One way ANOVA with Tukey's post-test (n=3) *p<0.05.

Establishing Sorafenib concentration in 2D versus 3D BME-2 culture :

To establish the effect of increasing concentration of Sorafenib in reducing viability of SNU-449 HCC line and LX-2 viability in 2D (plastic) and 3D BME2 matrix culture. SNU-449 HCC line and LX-2 were seeded individually at density of 2000 cell per well in 96-well plates, and for the 3D researcher add 40 µl Basement Membrane Extract 2 (BME-2) in allocate wells to form 3D structure. After overnight incubation cells were treated with 5, 10 20 or 50 µM Sorafenib dissolved in DMSO (0.5%). Cells treated with DMSO (0.5%) were used as a vehicle control for the experiment. Cells incubated for 72 hours of treatment and analyzed using cell viability assays CellTitre Glo3D. Researcher observed a reduction in SNU-449 cells (BME-2) viability of 16.8% (5 µM), 91.3% (10 µM), 91.9% (20 µM) and 98.7% (50 µM), and in SNU-449 cells (2D) of 2.7% (5 µM), 89.6% (10 µM), 91.1% (20 µM) and 99% (50 µM) treatment with Sorafenib (Figure 2A). In LX-2 cells (BME-2) viability reduction of 81.7% (5 µM), 93.9% (10 µM), 98.9% (20 µM) and 99.5% (50 µM) and in LX-2 cells (2D) of 86.7% (5 µM), 93.3% (10 µM), 92.4% (20 µM) and 99.4% (50 µM) treatment with Sorafenib (Figure 2B). Thus, researcher successfully established that Sorafenib effect cell viability and significantly reduced SNU-449 and LX-2 cells viability on both 2D and 3D models.
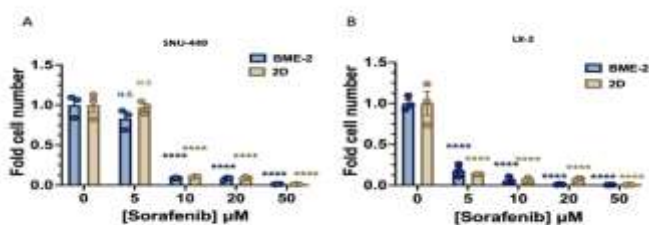

Figure 1. Effects of increase Sorafenib concentration on SNU-449 and LX-2 cells in 2-dimensional plastic (2D) versus 3-dimensional (3D) BME-2 matrix culture.

Cells were seeded and grown on plastic cell culture wells or seeded onto BME-2 matrix and treated with increasing concentrations of Sorafenib for 72 hours. Viability was quantified using CellTiter Glo3D reagent. **(A)** Quantification of SNU-449 HCC cell viability with increasing concentration of Sorafenib. Data are presented as a fold change over vehicle control and represent mean ± SEM (n=3). One way ANOVA with Tukey's post-test (n=3). N.S= No significance, ****p<0.0001. **(B)** Quantification of LX-2 hepatic stellate cell viability with increasing concentration of Sorafenib. Data are presented as a fold change over vehicle control and represent mean ± SEM (n=3). One way ANOVA with Tukey's post-test (n=3). ****p<0.0001.

Establishing Sorafenib concentration effect in 3D BME-2 matrix & 3D bio-printed versus 2D using RASTRUM bio-printer

To quantitate SNU-449 viability with increasing concentration of Sorafenib in 3D BME-2 matrix and 3D bio-printed versus 2D (on inert) and (on plastic) using a bio-printer. SNU-449 HCC line was seeded at density of 2000 cells per well in 96-well plate onto allocated wells using RASTRUM bio-printer and added 40 µl of BME-2 matrix in allocate wells to form 3D structure.

After overnight incubation cells were treated with 5, 10 20 or 50 µM Sorafenib dissolved in DMSO (0.5%). Cells treated with DMSO (0.5%) were used as a vehicle control for the experiment. Cells incubated for 72 hours of treatment and analyzed using cell viability assays CellTitre Glo3D. Researcher observed a reduction in SNU-449 cells 3D (bio-printed) viability of 29.8% (5 µM), 75.9% (10 µM), 84.5% (20 µM) and 90.5% (50 µM) and in SNU-449 3D (BME-2) matrix of 0% (5 µM), 69.1% (10 µM), 67.7% (20 µM) and 92.5% (50 µM) treatment with Sorafenib (Figure 3A). Versus, in 2D on (inert), SNU-449 cells viability reduction of 79.9% (5 µM), 77% (10 µM), 83.4% (20 µM) and 90.7% (50 µM), and in 2D on (plastic) viability reduction of 95.6% (5 µM), 89.4% (10 µM), 93.6% (20 µM) and 98.9% (50 µM) treatment with Sorafenib (Figure 3A).

Researcher successfully established that the concentration of Sorafenib between 5 and 50 µM significantly reduced SNU-449 HCC line viability. Thus, researcher determined the concentration dilution series of Sorafenib using a bio-printer for subsequent experiments.
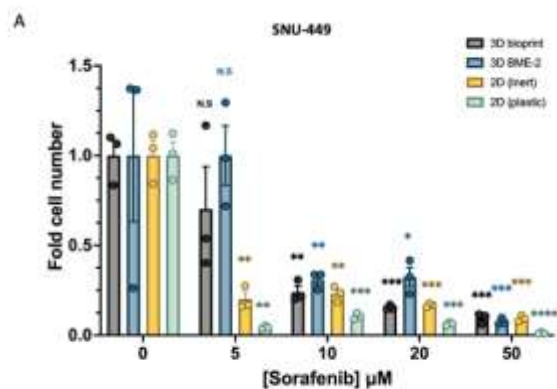

Figure 3. Effects of increase Sorafenib concentration on SNU-449 cells in 3D BME-2 matrix & 3D bio-printed versus 2D on inert and on plastic using RASTRUM bio-printer.

Cells were bio-printed and grown on culture wells and onto BME-2 matrix and treated with increasing concentrations of Sorafenib for 72 hours. **(A)** shows the reduction of SNU-449 viability in increasing concentration of Sorafenib as shows to inhibit SNU-449 cells viability in 3D bio-printed, 3D BME-2 matrix, 2D on (inert) & 2D on (plastic). Data are presented as a fold change over vehicle control and represent mean ± SEM (n=3). Two-way ANOVA with Tukey's post-test (n=3). N.S.= No significance, *p<0.05, **p<0.01, ***p<0.001, ****p<0.0001

Establishing Sorafenib concentration effect in a multi-cellular model using RASTRUM bio-printer

To quantitate the effect of increase Sorafenib concentration on a multi-cellular viability in 3D BME-2 matrix and 3D bio-printed versus 2D (on inert) and (on plastic) on SNU-449 and LX-2 cells combined at the ratio of (1:3). Researcher seeded 2000 cells per

well in 96-well plate using RASTRUM bio-printer and added 40 µl of BME-2 matrix in allocate wells to form 3D structure. After overnight incubation cells were treated with 5, 10 20 or 50 µM Sorafenib dissolved in DMSO (0.5%).

Cells treated with DMSO (0.5%) were used as a vehicle control for the experiment. Cells incubated for 72 hours of treatment and analyzed using cell viability assays CellTitre Glo3D. Researcher observed a reduction in SNU-449 and LX-2 cells combined in 3D (bio-printed) viability of 76.2% (5 µM), 91.5% (10 µM), 96.1% (20 µM) and 97.8% (50 µM) and in SNU-449 and LX-2 cells combined in 3D (BME-2) matrix of 82.3% (5 µM), 89.9% (10 µM), 92.5% (20 µM) and 96.9% (50 µM) treatment with Sorafenib (Figure 1A). Versus, in 2D on (inert), combined cells viability reduction of 87% (5 µM), 88.7% (10 µM), 91% (20 µM) and 95.4% (50 µM) and in 2D on (plastic) viability reduction of 93.1% (5 µM), 86.7% (10 µM), 91.2% (20 µM) and 97.5% (50 µM) treatment with Sorafenib (Figure 4A). Researcher successfully established that the concentration of Sorafenib between 5 and 50 µM significantly reduced SNU-449 and LX-2 combined cell viability. Researcher therefore successfully established the effect of Sorafenib in defined matrices for use in high-throughput drug screening.
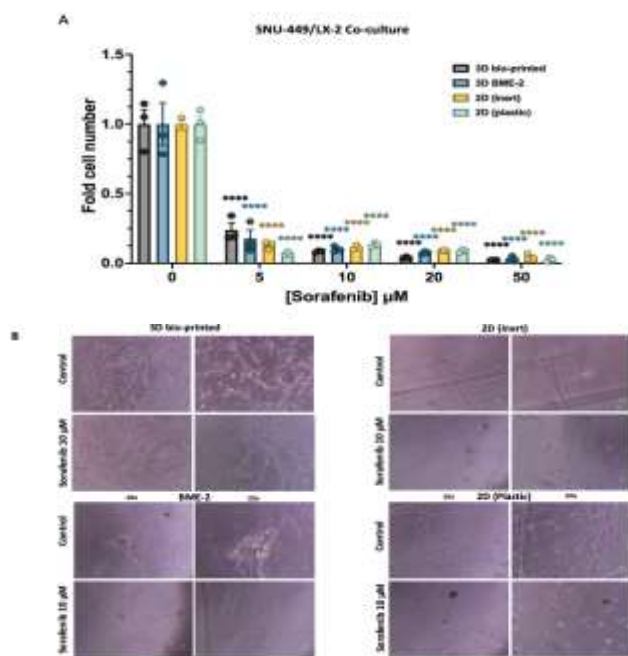

Figure 4. Effects of increase Sorafenib concentration on a multi-cellular model SNU-449 & LX-2 cells combined in 3D BME-2 matrix & 3D bio-printed versus 2D on inert and on plastic using RASTRUM bio-printer.
Cells were bio-printed and grown on culture wells and onto BME-2 matrix and treated with increasing concentrations of Sorafenib for 72 hours. **(A)** shows the reduction of bio-printed SNU-449 & LX-2 co-cultured cells viability in increasing concentration of Sorafenib as shows to inhibit cell viability 3D bio-printed, BME-2 3D, 2D (inert) & 2D (on plastic). Data are presented as a fold change over vehicle control and represent mean ± SEM (n=3). Two-way ANOVA with Tukey's post-test (n=3). ****p<0.0001. **(B)** Represent untreated and treated SNU-449 & LX-2 co-cultured cells in 3D bio-printed, BME-2 3D, 2D (inert) & 2D (on plastic).

DISCUSSION:

In this study researcher demonstrated that three-dimensional (3D) culture and two-dimensional (2D) culture responses effectively to Sorafenib. Then researcher assessed response to Sorafenib with interaction between HCC cells and CAFs to create HCC microenvironment in three-dimensional (3D) culture in the non-defined matrix BME2, and a novel bio-printed 3D models using defined matrices developed by Inventia Life Sciences.

Researcher successfully established a defined 3D culture system of a new bio-printed HCC model that reflect the interaction between cells more accurately and have more advantages comparable to BME-2 and 2D culture cells, which may aid in the advancement of drug discovery and personalized medicine.

Cancer drug discovery has been hampered by the lack of appropriate preclinical testing methods and in vitro models that are unable to accurately mimic the in vivo environment. Also, the heterogeneity of tumor microenvironment (TME) that affected by internal cell factors, cell interactions and cell microenvironment causing drug resistances (Zhu et al., 2021).

In most cancer treatments, tumours are treated as a homogeneous disease, based on that, efficacy of treatments varies in patients (Tang et al., 2020).

Accordingly, understanding these causes of drug resistance requires the development of preclinical testing methods and in vitro model that reflect the tumor heterogeneity *in vivo in vitro*. Consequently, understanding cell-cell and cell-extracellular interactions in depth to increase the success rate of the drug development process could help to develop effective cancer treatments. For instance, 2D culture methods have several advantages such as low-cost maintenance, simplicity of culture and easy to interpret the results (Jensen, C., & Teng, Y.,2020).

However, the disadvantage of 2D culture is that this does not mimic the 3D environment of tissues and tumours, which contain complex cell-cell and cell-extracellular interaction. The importance of these interactions are the cellular regulation phenotype and behavior such as, cell migration, cell proliferation and differentiation (Sainio, A., & Järveläinen, H., 2020).

Conversely, 3D cultures methods have been showing great promise in modelling the functional pathology *of in vivo* tumours and in the innovation of drug discovery and screening (Fontana et al., 2021) (Rodrigues et al., 2021).

Thus, our aim was to develop a new bio-printed HCC model that more accurately models the microenvironment and includes interactions between HCC cells and CAFs. Therefore, researcher established a novel bio-printed 3D model of HCC composed of SNU449/LX-2 co-cultures using defined matrices developed by Inventia Life Sciences and researcher assessed responses to Sorafenib using viability analysis (figure-4).

Researcher show significance reduction of SNU449/LX-2 co-cultured cells viability in 3D models similarly in 2D models

(figure-4). Nonetheless, a multi-cellular model cultured in 2D model and grown in plastic to test drug efficacy consider imprecisely mimicking the tumor stroma (Law et al., 2021).

In results failure to develop an anti-cancer drug due to the insufficiency of appropriate preclinical in vitro models that do not represent the cellular effects of drugs and cell- extracellular and drug penetration ECM stiffness that influences cell behavior (Law et al., 2021).

Defined matrices researcher used contain components that are keys in extracellular matrix (ECM) protein, mainly are collagen (modelled by in our system GFOGER), hyaluronic acid and integrin-binding proteins (modelled by RGD in our system). Using these defined matrices more precisely models' cell-ECM interaction and cells response that is influenced by ECM stiffness. Thus, use of the defined matrices in co-culture benefit in mimicking the liver tumour microenvironment on cell-cell and cell-extracellular interaction more accurately (Habanjar et al., 2021) (Mazzocchi et al.,2018).

In comparison to another 3D matrix, Basement Membrane Extract 2 (BME-2) mainly composed of laminin and collagen with other undefined components. BME is used to expand the organoids and used as a replacement of ECM to mimic its function such as, influencing cell proliferation and differentiation. Although has been showing to sustain cells in undifferentiated and un-proliferative state in the liver due to the presence of laminin (Willemse et al., 2022).

CONCLUSION :

The most common culture method is 2D but owing to its limitations, 3D culture methods may open a whole new world of accurate drug response modelling to develop cancer therapies. Defined 3D cultures have huge advantage in their ability to precisely model cell interactions with their environment, reproducibly and accurately. Combining this with a multi-cellular culture will aid in replicating the complex microenvironment of HCC to facilitate drug research (Habanjar et al., 2021). Overall, overcoming the limitation of 3D culture with advancement of bioprinting would benefits in treatment of disease, drug toxicity testing and personalized medicine. As well as succeeding in developing *in vitro* model that reflect the pathophysiological histologically, biochemically, and functionally.

REFERENCES:

Arriazu, E., Ruiz de Galarreta, M., Cubero, F. J., Varela-Rey, M., Pérez de Obanos, M. P., Leung, T. M., Lopategi, A., Benedicto, A., Abraham-Enachescu, I., & Nieto, N. (2014). Extracellular matrix and liver disease. *Antioxidants & redox signaling*, *21*(7), 1078–1097. https://doi.org/10.1089/ars.2013.5697

Ayvaz, I., Sunay, D., Sariyar, E., Erdal, E., & Karagonlar, Z. F. (2021). Three-Dimensional Cell Culture Models of Hepatocellular Carcinoma - a Review. *Journal of gastrointestinal cancer*, *52*(4), 1294–1308. https://doi.org/10.1007/s12029-021-00772-1

Balakrishnan, S., Atal, S., Ray, A., Pravin, C. A., & Nanda, M. (2020). Organoids: An invaluable tool in pharmacology. *Indian journal of pharmacology*, *52*(5), 422–429. https://doi.org/10.4103/ijp.IJP_137_19

Bu, L., Baba, H., Yasuda, T., Uchihara, T., & Ishimoto, T. (2020). Functional diversity of cancer-associated fibroblasts in modulating drug resistance. *Cancer science*, *111*(10), 3468–3477. https://doi.org/10.1111/cas.14578

Cadamuro, M., Brivio, S., Spirli, C., Joplin, R. E., Strazzabosco, M., & Fabris, L. (2017). Autocrine and Paracrine Mechanisms Promoting Chemoresistance in Cholangiocarcinoma. *International journal of molecular sciences*, *18*(1), 149. https://doi.org/10.3390/ijms18010149

Dallavalasa, S., Beeraka, N. M., Basavaraju, C. G., Tulimilli, S. V., Sadhu, S. P., Rajesh, K., Aliev, G., & Madhunapantula, S. V. (2021). The Role of Tumor Associated Macrophages (TAMs) in Cancer Progression, Chemoresistance, Angiogenesis and Metastasis - Current Status. *Current medicinal chemistry*, *28*(39), 8203–8236. https://doi.org/10.2174/0929867328666210720143721

Dasgupta, P., Henshaw, C., Youlden, D. R., Clark, P. J., Aitken, J. F., & Baade, P. D. (2020). Global Trends in Incidence Rates of Primary Adult Liver Cancers: A Systematic Review and Meta-Analysis. *Frontiers in oncology*, *10*, 171. https://doi.org/10.3389/fonc.2020.00171

Dwyer, B. J., Macmillan, M. T., Brennan, P. N., & Forbes, S. J. (2021). Cell therapy for advanced liver diseases: Repair or rebuild. *Journal of hepatology*, *74*(1), 185–199. https://doi.org/10.1016/j.jhep.2020.09.014

Elpek G. Ö. (2014). Cellular and molecular mechanisms in the pathogenesis of liver fibrosis: An update. *World journal of gastroenterology*, *20*(23), 7260–7276. https://doi.org/10.3748/wjg.v20.i23.7260

Farzaneh, Z., Vosough, M., Agarwal, T., & Farzaneh, M. (2021). Critical signaling pathways governing hepatocellular carcinoma behavior; small molecule-based approaches. *Cancer cell international*, *21*(1), 208. https://doi.org/10.1186/s12935-021-01924-w

Feng, B., Wu, J., Shen, B., Jiang, F., & Feng, J. (2022). Cancer-associated fibroblasts and resistance to anticancer therapies: status, mechanisms, and countermeasures. *Cancer cell international*, *22*(1), 166. https://doi.org/10.1186/s12935-022-02599-7

Fontana, F., Marzagalli, M., Sommariva, M., Gagliano, N., & Limonta, P. (2021). In Vitro 3D Cultures to Model the Tumor Microenvironment. *Cancers*, *13*(12), 2970. https://doi.org/10.3390/cancers13122970

Gomaa, A. I., Khan, S. A., Toledano, M. B., Waked, I., & Taylor-Robinson, S. D. (2008). Hepatocellular carcinoma: epidemiology, risk factors and pathogenesis. *World journal of gastroenterology*, *14*(27), 4300–4308. https://doi.org/10.3748/wjg.14.4300

Gunaydin G. (2021). CAFs Interacting With TAMs in Tumor Microenvironment to Enhance Tumorigenesis and Immune Evasion. *Frontiers in oncology*, *11*, 668349. https://doi.org/10.3389/fonc.2021.668349

Habanjar, O., Diab-Assaf, M., Caldefie-Chezet, F., & Delort, L. (2021). 3D Cell Culture Systems: Tumor Application, Advantages, and Disadvantages. *International journal*

of molecular sciences, *22*(22), 12200. https://doi.org/10.3390/ijms222212200

Hernandez-Gea, V., Toffanin, S., Friedman, S. L., & Llovet, J. M. (2013). Role of the microenvironment in the pathogenesis and treatment of hepatocellular carcinoma. *Gastroenterology*, *144*(3), 512–527. https://doi.org/10.1053/j.gastro.2013.01.002

Hou, X. J., Ye, F., Li, X. Y., Liu, W. T., Jing, Y. Y., Han, Z. P., & Wei, L. X. (2018). Immune response involved in liver damage and the activation of hepatic progenitor cells during liver tumorigenesis. *Cellular immunology*, *326*, 52–59. https://doi.org/10.1016/j.cellimm.2017.08.004

Jensen, C., & Teng, Y. (2020). Is It Time to Start Transitioning From 2D to 3D Cell Culture?. *Frontiers in molecular biosciences*, *7*, 33. https://doi.org/10.3389/fmolb.2020.00033

Kanzaki, R., & Pietras, K. (2020). Heterogeneity of cancer-associated fibroblasts: Opportunities for precision medicine. *Cancer science*, *111*(8), 2708–2717. https://doi.org/10.1111/cas.14537

Krenkel, O., & Tacke, F. (2017). Liver macrophages in tissue homeostasis and disease. *Nature reviews. Immunology*, *17*(5), 306–321. https://doi.org/10.1038/nri.2017.11

Kumari, R., Sahu, M. K., Tripathy, A., Uthansingh, K., & Behera, M. (2018). Hepatocellular carcinoma treatment: hurdles, advances and prospects. *Hepatic oncology*, *5*(2), HEP08. https://doi.org/10.2217/hep-2018-0002

Law, A., Rodriguez de la Fuente, L., Grundy, T. J., Fang, G., Valdes-Mora, F., & Gallego-Ortega, D. (2021). Advancements in 3D Cell Culture Systems for Personalizing Anti-Cancer Therapies. *Frontiers in oncology*, *11*, 782766. https://doi.org/10.3389/fonc.2021.782766

Li, X. Y., Yang, X., Zhao, Q. D., Han, Z. P., Liang, L., Pan, X. R., Zhu, J. N., Li, R., Wu, M. C., & Wei, L. X. (2017). Lipopolysaccharide promotes tumorigenicity of hepatic progenitor cells by promoting proliferation and blocking normal differentiation. *Cancer letters*, *386*, 35–46. https://doi.org/10.1016/j.canlet.2016.10.044

Linares, J., Marín-Jiménez, J. A., Badia-Ramentol, J., & Calon, A. (2021). Determinants and Functions of CAFs Secretome During Cancer Progression and Therapy. *Frontiers in cell and developmental biology*, *8*, 621070. https://doi.org/10.3389/fcell.2020.621070

Liu, J., Li, P., Wang, L., Li, M., Ge, Z., Noordam, L., Lieshout, R., Verstegen, M., Ma, B., Su, J., Yang, Q., Zhang, R., Zhou, G., Carrascosa, L. C., Sprengers, D., IJzermans, J., Smits, R., Kwekkeboom, J., van der Laan, L., Peppelenbosch, M. P., … Cao, W. (2021). Cancer-Associated Fibroblasts Provide a Stromal Niche for Liver Cancer Organoids That Confers Trophic Effects and Therapy Resistance. *Cellular and molecular gastroenterology and hepatology*, *11*(2), 407–431. https://doi.org/10.1016/j.jcmgh.2020.09.003

Liu, T., Han, C., Wang, S., Fang, P., Ma, Z., Xu, L., & Yin, R. (2019). Cancer-associated fibroblasts: an emerging target of anti-cancer immunotherapy. *Journal of hematology & oncology*, *12*(1), 86. https://doi.org/10.1186/s13045-019-0770-1

Mazzocchi, A., Devarasetty, M., Huntwork, R., Soker, S., & Skardal, A. (2018). Optimization of collagen type I-hyaluronan hybrid bioink for 3D bioprinted liver microenvironments. *Biofabrication*, *11*(1), 015003. https://doi.org/10.1088/1758-5090/aae543

McGlynn, K. A., Petrick, J. L., & El-Serag, H. B. (2021). Epidemiology of Hepatocellular Carcinoma. *Hepatology (Baltimore, Md.)*, *73 Suppl 1*(Suppl 1), 4–13. https://doi.org/10.1002/hep.31288

Nuciforo, S., & Heim, M. H. (2020). Organoids to model liver disease. *JHEP reports : innovation in hepatology*, *3*(1), 100198. https://doi.org/10.1016/j.jhepr.2020.100198

Park, J. G., Lee, J. H., Kang, M. S., Park, K. J., Jeon, Y. M., Lee, H. J., Kwon, H. S., Park, H. S., Yeo, K. S., & Lee, K. U. (1995). Characterization of cell lines established from human hepatocellular carcinoma. *International journal of cancer*, *62*(3), 276–282. https://doi.org/10.1002/ijc.2910620308

Prieto, J., Melero, I., & Sangro, B. (2015). Immunological landscape and immunotherapy of hepatocellular carcinoma. *Nature reviews. Gastroenterology & hepatology*, *12*(12), 681–700. https://doi.org/10.1038/nrgastro.2015.173

Ringelhan, M., Pfister, D., O'Connor, T., Pikarsky, E., & Heikenwalder, M. (2018). The immunology of hepatocellular carcinoma. *Nature immunology*, *19*(3), 222–232. https://doi.org/10.1038/s41590-018-0044-z

Rodrigues, J., Heinrich, M. A., Teixeira, L. M., & Prakash, J. (2021). 3D In Vitro Model (R)evolution: Unveiling Tumor-Stroma Interactions. *Trends in cancer*, *7*(3), 249–264. https://doi.org/10.1016/j.trecan.2020.10.009

Sainio, A., & Järveläinen, H. (2020). Extracellular matrix-cell interactions: Focus on therapeutic applications. *Cellular signalling*, *66*, 109487. https://doi.org/10.1016/j.cellsig.2019.109487

Seki, E., & Schwabe, R. F. (2015). Hepatic inflammation and fibrosis: functional links and key pathways. *Hepatology (Baltimore, Md.)*, *61*(3), 1066–1079. https://doi.org/10.1002/hep.27332

Sung, H., Ferlay, J., Siegel, R. L., Laversanne, M., Soerjomataram, I., Jemal, A., & Bray, F. (2021). Global Cancer Statistics 2020: GLOBOCAN Estimates of Incidence and Mortality Worldwide for 36 Cancers in 185 Countries. *CA: a cancer journal for clinicians*, *71*(3), 209–249. https://doi.org/10.3322/caac.21660

Tang, W., Chen, Z., Zhang, W., Cheng, Y., Zhang, B., Wu, F., Wang, Q., Wang, S., Rong, D., Reiter, F. P., De Toni, E. N., & Wang, X. (2020). The mechanisms of sorafenib resistance in hepatocellular carcinoma: theoretical basis and therapeutic aspects. *Signal transduction and*

targeted therapy, *5*(1), 87. https://doi.org/10.1038/s41392-020-0187-x

Tang, W., Chen, Z., Zhang, W., Cheng, Y., Zhang, B., Wu, F., Wang, Q., Wang, S., Rong, D., Reiter, F. P., De Toni, E. N., & Wang, X. (2020). The mechanisms of sorafenib resistance in hepatocellular carcinoma: theoretical basis and therapeutic aspects. *Signal transduction and targeted therapy*, *5*(1), 87. https://doi.org/10.1038/s41392-020-0187-x

Vannella, K. M., & Wynn, T. A. (2017). Mechanisms of Organ Injury and Repair by Macrophages. *Annual review of physiology*, *79*, 593–617. https://doi.org/10.1146/annurev-physiol-022516-034356

Willemse, J., van der Laan, L., de Jonge, J., & Verstegen, M. (2022). Design by Nature: Emerging Applications of Native Liver Extracellular Matrix for Cholangiocyte Organoid-Based Regenerative Medicine. *Bioengineering (Basel, Switzerland)*, *9*(3), 110. https://doi.org/10.3390/bioengineering9030110

Wu, F., Yang, J., Liu, J., Wang, Y., Mu, J., Zeng, Q., Deng, S., & Zhou, H. (2021). Signaling pathways in cancer-associated fibroblasts and targeted therapy for cancer. *Signal transduction and targeted therapy*, *6*(1), 218. https://doi.org/10.1038/s41392-021-00641-0

Xu, L., Hui, A. Y., Albanis, E., Arthur, M. J., O'Byrne, S. M., Blaner, W. S., Mukherjee, P., Friedman, S. L., & Eng, F. J. (2005). Human hepatic stellate cell lines, LX-1 and LX-2: new tools for analysis of hepatic fibrosis. *Gut*, *54*(1), 142–151. https://doi.org/10.1136/gut.2004.042127

Yang, Q., Guo, N., Zhou, Y., Chen, J., Wei, Q., & Han, M. (2020). The role of tumor-associated macrophages (TAMs) in tumor progression and relevant advance in targeted therapy. *Acta pharmaceutica Sinica. B*, *10*(11), 2156–2170. https://doi.org/10.1016/j.apsb.2020.04.004

Zhu, L., Jiang, M., Wang, H., Sun, H., Zhu, J., Zhao, W., Fang, Q., Yu, J., Chen, P., Wu, S., Zheng, Z., & He, Y. (2021). A narrative review of tumor heterogeneity and challenges to tumor drug therapy. *Annals of translational medicine*, *9*(16), 1351. https://doi.org/10.21037/atm-21-1948